Environmental Earth Sciences (2021) 80:555
https://doi.org/10.1007/s12665-021-09849-3

ORIGINAL ARTICLE

Indoor radon concentration and a diffusion model in dwellings situated in a subalkaline granitoid area, Southern Brazil

G. Romero-Mujalli[1,2] · A. Roisenberg[3] · A. Cordova-Gonzalez[1] · P. H. P. Stefano[3]

Received: 22 October 2020 / Accepted: 30 July 2021 / Published online: 16 August 2021

Abstract

Radon (Rn), a radioactive element, has especial interest in medical geology because long-term exposure to high concentration is related to lung cancer. In this study, outdoor and indoor radon measurements were conducted in dwellings of the Piquiri Syenite Massif, located in southern Brazil, given the relative high Rn content in soils of this region. Measurements were done using CR-39 detectors and placing them inside and outside dwellings. Moreover, a one-dimensional diffusion model was performed in order to quantify the natural transport of Rn to the air in confined and aerated environments. Results indicate that the region presents relatively low air Rn concentrations, within the environmental limits; however, the health risk might increase in confined and ill-ventilated environments because of transfer from soil and exhalation from ornamental rock-material often found inside dwellings. The main north facies of the syenite, where most of the rock extractions are located, was found to have the highest air Rn concentration because of the higher soil Rn concentration, compared to other facies of the syenite.

Keywords Radon · Syenite · Radioactivity · Diffusion model

Introduction

Radon (Rn) is a noble gas found in the atmosphere, trapped between soil grains and dissolved in water. Unlike other noble gases, Rn does not have stable isotopes; instead, all of its isotopes are radioactive. There are three naturally occurring isotopes of radon, each one associated with a different radioactive decay series, ^{222}Rn (radon), which occurs in the ^{238}U series, ^{220}Rn (thoron) in the ^{232}Th series and ^{219}Rn (actinon) in the ^{235}U series. Their direct parent atoms are ^{226}Ra, ^{224}Ra and ^{223}Ra, respectively (Sextro 1994; Ferronsky and Polyakov 2012).

✉ G. Romero-Mujalli
gibran.mujalli@gmail.com

1 Institut Für Geologie, Centrum Für Erdsystemforschung Und Nachhaltigkeit (CEN), Universität Hamburg, Bundesstraße 55, 20146 Hamburg, Germany

2 Instituto de Ciencias de La Tierra, Facultad de Ciencias, Universidad Central de Venezuela, Caracas, Venezuela

3 Departamento de Mineralogia E Petrologia, Instituto de Geociências, Universidade Federal Do Rio Grande Do Sul, Av. Bento Gonçalves, 9500, CEP 91540-000 Porto Alegre, RS, Brasil

The occurrence and abundance of radioisotopes in nature depend on the instability of the atom, characterized by the half-life time, which is the time required for the concentration of a radionuclide to decay by a one-half of its initial concentration. ^{222}Rn has a 3.82 days half-life, while ^{220}Rn and ^{219}Rn have very short half-life (56 and 3.92 s, respectively), limiting the indoor concentration of these two isotopes and its decay products, especially for the latter isotope because of the naturally low abundance of the ^{235}U precursor (Sextro 1994; Appleton 2005). Therefore, ^{222}Rn is the most abundant radon isotope in nature, transported along higher distances than the other Rn isotopes. Its occurrence is related with the mobility of ^{226}Ra, which at the same time is related with the geochemical behavior of ^{238}U (Appleton 2005).

The decay series of ^{238}U, ^{232}Th, ^{235}U end with the formation of stable isotopes of ^{206}Pb, ^{208}Pb and ^{207}Pb, respectively (Sextro 1994; Ferronsky and Polyakov 2012). The radioactive decays proceed either by alpha decay, in which the unstable nucleus emits an alpha particle, equivalent to a ^{4}He nucleus, or beta decay, in which the unstable nucleus emits an electron or a positron (Sextro 1994). Decay can also lead to the emission of gamma radiation, which exposure can be dangerous to humans. Several studies conducted by health organizations such as WHO (World Health Organization

2009) are focused on environmental impact of Rn to human health and it has been well established that exposure to Rn causes lung cancer. Nevertheless, the risks due to Rn are not fully recognized by the people (Nagda 1994).

Radon is the only element in gas state formed from the decay series of ^{238}U, ^{232}Th and ^{235}U, which are common elements in soils and rocks, being continually produced, from where it can migrate through fractures to reach a fluid phase (water or air). High concentrations of this element in the air are related to occurrence of igneous rocks with alkaline affinity, carbonaceous shales, carbonate rocks and phosphate rocks that present higher concentrations of uranium and radium. In granitic and syenitic rocks, minerals such as zircon, apatite, monazite and others present high radon contents (Appleton 2005). The emanation rate of radon depends on uranium concentration in soil or rock mineralogy. Mineral solubility, grain size and mineral internal structure are main factors affecting the release of Rn to the atmosphere. Therefore, it is expected that soils release more Rn than rocks (Appleton 2005).

Most of the Rn released to the atmosphere does not represent a risk to human health. However, Rn can be accumulated inside buildings, caves and mines, due to low air exchange rate, affecting the health of those who have constant exposure with these environments. Consequently, high radon concentrations in closed environments are responsible of causing lung cancer in the population. The World Health Organization (2009) has established that for residences and public buildings the reference indoor Rn concentration per year is 100 Bq m^{-3}, recommending a maximum limit of 300 Bq m^{-3}. On the other hand, the USEPA (2016) set an action level of 148 Bq m^{-3} (4 pCi L^{-1}). The International Atomic Energy Agency (2014) has established that in workplaces such as underground mines, the maximum concentration is 1000 Bq m^{-3}.

In Brazil, lung cancer is one of the most important causes of high mortality rates (Castro et al. 2004). In recent years, some studies have been developed to determine the concentrations of radon in underground mines, groundwater, soil and air (Buffon 2002; Silva 2005; Santos 2008; Fianco et al. 2013; Romero-Mujalli and Roisenberg 2016).

One of the most common devices implemented to determine indoor Rn concentrations is the use of plastic detectors. However, they often require relative longer measuring time for monitoring purpose. Therefore, new techniques have been studied: predicting the indoor Rn concentrations based on air change rate (McGrath and Byrne 2020); by using continuous real-time air quality monitoring devices (Tunyagi et al. 2020); or by predicting potential Rn concentration based on geology, exhalation rates and characteristic of dwellings (Casey et al. 2015; Florică et al. 2020; Haneberg et al. 2020). The latter is the most common applicable, not only because of the lower cost compared with the other techniques, but given that it studies the source of Rn, which depends on type of rock and determined the potential accumulation in dwellings. The present study area represents an intrusion of rocks with alkaline affinity and high concentrations of uranium and large-ion lithophile elements (LILE) such as Rb and Cs (Nardi et al. 2007). These rocks have been used in construction business and most of this material goes to the international market. Romero-Mujalli and Roisenberg (2016) studied the natural radiation in soils of this region, measuring the Rn concentration in different facies of the syenite massif. It was concluded that the high Rn concentration in soils might represent a risk to the health of the inhabitants of the regions. The present study aims to quantify the indoor Rn concentration and its relation to the outdoor concentration for different facies of the syenite massif. In addition, a diffusion model is presented which allows the calculation of indoor and outdoor Rn concentration expected in confined and ventilated (aerated) environments in direct contact with the soil. Given the relatively high Rn concentrations in soils of this region, the measured outdoor Rn concentration is compared to the simulation results, in order to identify the main mechanism controlling Rn concentration in air (outdoor).

Material and methods

Study area and geological setting

The study area is located in the central-East region of the State of *Rio Grande do Sul*, Southern Brazil, where the Piquiri Syenite Massif (PSM) outcrops (Fig. 1). This area is characterized by a subtropical humid climate, with average temperature of about 18 °C and annual precipitation of approximately 1700 mm (Instituto Nacional de Meteorologia (INMET 2020)). This area is represented by the Sul-Riograndense Shield, which is the result of production and deformation of continental crust taken place in Transamazonian and Brazilian Orogeny (760–550 Ma). The last orogeny cycle has produced a geological unit named Pelotas Batholith, representing a period of crustal reworking, constituted by six granitic suites and the Piquiri Syenite Massif (Philipp et al. 2002; Hartmann et al. 2007), which is a semicircular intrusion with an approximately area of 150 km^2 and age of 611 Ma ± 3 Ma (Philipp et al. 2002). This intrusion is represented by three main lithological facies with gradual contacts (Fig. 2). The main facies represents the main part of the intrusion with a predominance of alkali feldspar syenite with a coarse equigranular texture, while the border facies is composed by fine syenites and quartz monzonite rocks of fine grained texture. The third type, located in the centre of the intrusion, varies between alkali feldspar granites and syenogranites. Moreover, phlogopite-bearing alkali feldspar

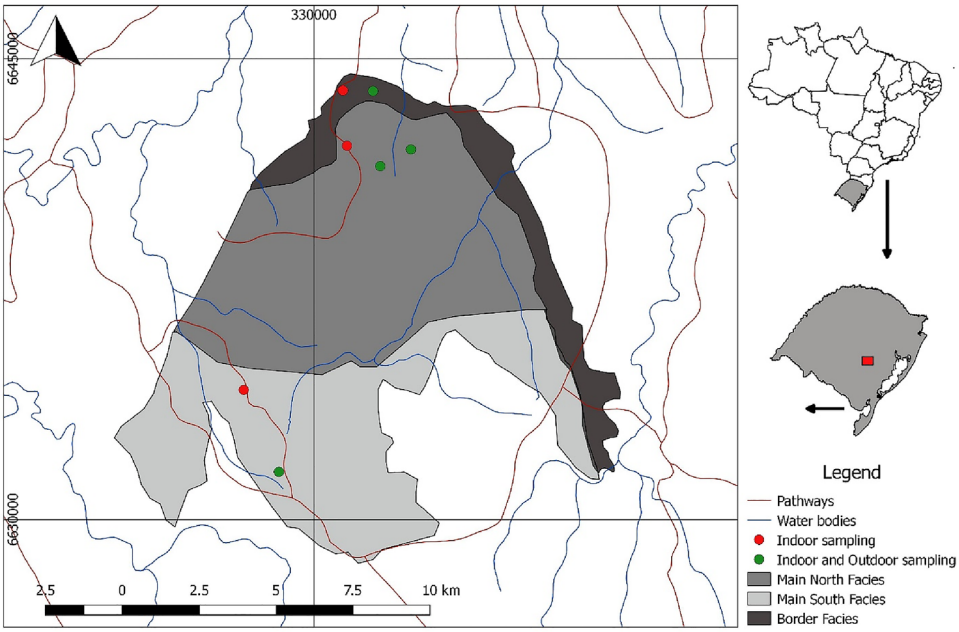

Fig. 1 Map representation of the study area. The shadowed region represents the limits of the Piquiri Syenite Massif

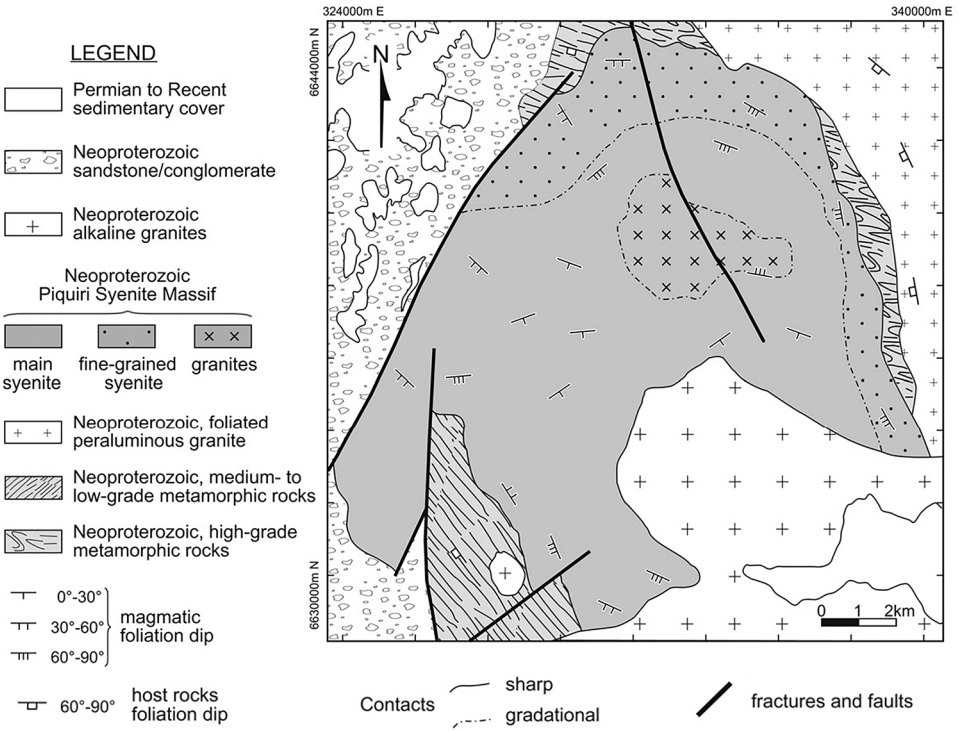

Fig. 2 Geological map of the Piquiri Syenite Massif (Nardi et al. 2008)

syenites has been described as showing mingling features with the alkali feldspar syenites (Nardi et al. 2007, 2008).

CR-39 radon detectors

The detection of Rn in air was made using Allyl Diglycol carbonate (ADC; $C_{12}H_{18}O_7$), a polymer made from the monomer CR-39, Columbia Resin #39 (Kukreja et al. 1984). These detectors are colourless, with a density of 1.30 g cm^{-3} and a thickness of 1.0 mm. As the gas starts to penetrate in the chamber, the decay of radon and its descendants is seen as microscopic tracks. These tracks are results of the interaction of alpha particles with the detector material (Pereira et al. 1983). Given that most of the dwellings in this region are private, the placement of detectors were done after confirming permission from owners. In total, 12 sample points

(8 indoors and 4 outdoors) were established to measure radon concentration in air, covering three difference regions of the Piquiri Syenite Massif, one associated to the border and the other two to the main facies (north and south), based on in situ soil Rn measurements using the AlphaGUARD PQ 2000 PRO equipment (Romero-Mujalli and Roisenberg 2016), which found that main north facies is concentrated in ^{222}Rn, whereas in the main south facies the ^{220}Rn isotope is dominant. Therefore, eleven CR-39 detectors were distributed along the intrusion, divided by three types according to the syenitic facies: main north (MN), main south (MS) and border facies (B).

The detectors were placed in the ground floor for all sampling locations. After 168 to 169 days, the CR-39 detectors were collected and etched in a 30% KOH at 80 °C for 6 h. The track density was measured in laboratory by optical microscopy and related to the radon concentration through the following equation:

$$C_{\mathrm{Rn}} = \frac{d}{St} \tag{1}$$

where d is the track density (track cm^{-2}), S is the detector sensitivity equivalent to 2.8 ± 0.2 (track cm^{-2} per kBq h. m^{-3}), and t is the sampling time (hours).

One-dimensional diffusion model

A Rn diffusion model from soil to air was constructed based on soil Rn concentration (Romero-Mujalli and Roisenberg 2016), in order to quantify the predicted indoor Rn concentrations for each syenite massif facies (northern main facies, southern main facies and border facies). Two model settings were carried out, one without any air exchange rate and the other including an air exchange rate. Table 1 summarizes the parameters implemented in the diffusion model. We conducted a Monte-Carlo approach, each simulation was calculated 1000 times, to assess uncertainty propagation. The results were compared with the measured indoor and outdoor Rn concentration obtained in this work for each facies of the Syenite Massif.

The diffusion of Rn through porous medium is described by Fick's law as:

$$J = -D\frac{\partial C_{(x,t)}}{\partial x} \tag{2}$$

where J stands for the radon flux density (Bq m^{-2}), D is the diffusion coefficient in the medium (m^2 s^{-1}) and $C_{(x,t)}$ is the Rn concentration (Bq m^{-3}). This equation describes the diffusion flux from high to low concentration along the x dimension dependent on time t. Moreover, the differential equation for the one dimension diffusion in two different mediums is:

Table 1 Configuration and parameters used to build the diffusion model

Parameter/variable	Symbol	Value
Number of random calculations	N	1000
Porosity	Θ	0.5 ± 0.2 m^3 m^{-3}
Moisture saturation	m	From 0.3 to 0.55
^{222}Rn decay constant	$\lambda 222$	2.0984×10^{-6} s^{-1}
^{220}Rn decay constant	$\lambda 220$	1.242×10^{-2} s^{-1}
Air diffusion coefficient	$Dair$	1×10^{-5} m^2 s^{-1}
Maximum height of model	$Xmax$	2 m
Minimum height of model	$Xmin$	-0.5 m
Interface Soil-Air	x_0	0 m
Grid size	Dx	0.01 m
Time step	Dt	60 s
Simulation time	T	24 h
Ventilation rate or air exchange rate	V	1×10^{-5} and 8×10^{-4} s^{-1}

Deviation for air exchange rate was taken to be 50%. Air exchange rates were set based on Andersen (2001) and Chao et al. (1997)

$$\frac{\partial C_{(x,t)}}{\partial t} = D\frac{\partial^2 C_{(x,t)}}{\partial x^2} - \lambda C_{(x,t)} + P_{(x)} - vC_{(x,t)} \tag{3}$$

where λ is the decay constant of radon (2.0984×10^{-6} s^{-1} for ^{222}Rn and 1.242×10^{-2} s^{-1} for ^{220}Rn), $P_{(x)}$ the production rate of radon in the media and v represent the air exchange rate (or ventilation rate in s^{-1}). For the present model, a production rate equals to the radioactivity decay ($\lambda C[x,t]$) was considered in the soil medium for $x \leq x_0$—dx, in order to neutralize the effect of radioactive decay in the soil, with the exception of the boundary between the air and the soil. Moreover, the production rate in air was set equal to 0 because all the Rn is released from minerals which are contained in the soil and in the PSM rocks.

The initial conditions of concentration of Rn in air were set as 0, and the concentration in the soil was set following the measured concentrations (Romero-Mujalli and Roisenberg 2016), summarized in Table 2. The upper (at $x_{\max}$) and bottom ($x_{\min}$) boundary conditions were established equal as the adjacent point as $C_{(x\max,t)} = C_{(x\max\text{-}1,t\text{-}1)}$ and $C_{(x\min,t)} = C_{\mathrm{soil}}$.

The radon flux density (Eq. 2) must be continuous across the boundary between soil and air, hence $J_{soil} = J_{air}$ at $x = 0$ (x_0, interface soil-air). And the concentration was calculated by:

$$C_{(x_0,t)} = \frac{D_{soil}C_{(x_0-dx,t)} + D_{air}C_{(x_0+dx,t)}}{D_{air} + D_{soil}} \tag{4}$$

The radon diffusion coefficient (D_{soil}) in soil was estimated using the equation provided by Rogers and Nielson (1991) which is written as follows:

Table 2 Mean values of soil radon concentrations (Romero-Mujalli and Roisenberg 2016) and air radon concentrations for each facies of the Piquiri Syenite Massif

Facies	Soil Rn conc. (kBq m^{-3})				Air Rn conc. (kBq m^{-3})	
	Total Rn	^{220}Rn	^{222}Rn	Relative air humidity in soil (%)	Outdoor	Indoor
Main north	300 ± 200	110 ± 100	200 ± 100	40 ± 6	0.009 ± 0.002	0.06 ± 0.06
Main south	300 ± 200	300 ± 200	5 ± 4	40 ± 10	0.0087 ± 0.0006	0.1 ± 0.1
Border	110 ± 70	60 ± 50	50 ± 30	45 ± 10	0.018 ± 0.001	0.03 ± 0.02

The given uncertainty represents the standard deviation calculated for each syenitic facies

$$D_{soil} = D_{air}\theta e^{-6m-6\left(\frac{m}{\theta}\right)^{14\theta}} \quad (5)$$

where D_{air} is the radon diffusion coefficient in air with value of 1×10^{-5} m^2 s^{-1}, θ is the porosity of the soil, and m is the volume fraction of moisture saturation in the soil. The porosity and the soil moisture fraction were randomly selected based on qualitative observations in field and assuming that the soil water content is proportional to the relative air humidity in soil at constant temperature.

A finite difference method (FDM) was performed to solve the diffusion equation, calculating the central difference for the derivative and using the Crank–Nicolson scheme to solve numerically. The simulations stored the information when a concentration of 0.1 kBq m^{-3} was reached at $x = 1.9$ m, in order to compare the time among the different facies studied. Moreover, a sensitivity test was conducted and a stochastic simulation was performed, establishing the confidence limit for simulations with air ventilation rate greater than 0 and simulations with no ventilation rate.

Results

Radon indoor results

The outdoor Rn concentration obtained using the CR-39 detectors varies between 0.008 and 0.018 kBq m^{-3} that might represent the natural concentration expected in the region. Indoor Rn concentration varies from 0.013 to 0.22 kBq m^{-3}. From seven indoor measurements, only two (1109 and 1112 detectors) exceed the public health reference level of 0.1 kBq m^{-3} recommended by World Health Organization (2009), with values of 0.22 and 0.11 kBq m^{-3}, located in the southern and northern main facies, respectively (Table 3). However, it is worth noticing that in this study all indoor Rn concentrations measured by CR-39 detectors are lower than the maximum recommended limit of 0.3 kBq m^{-3} (World Health Organization 2009), which is equivalent to 10 mSv a^{-1}. Moreover, the offices and stores are not frequently used, only during working hours of the

Table 3 Location of CR-39 detectors and air radon concentration for the main north (MN), south (MS) and border facies (B) of the Piquiri Syenite Massif

Code	Lon 22 J (mE)	Lat (mS)	Rn (kBq m^{-3})	Description	Facies	Height[a] (±0.1 m)	Set up date (dd.mm.yyyy)	Collected on (dd.mm.yyyy)
1116	331,297	6,644,080	0.048 ± 0.003	Indoor (living room)	B	1.7	14.10.2014	31.03.2015
1097	331,297	6,644,080	0.018 ± 0.001	Outdoor (open shed)	B	1.9	14.10.2014	31.03.2015
1101	330,887	6,643,962	0.013 ± 0.001	Indoor (living room)	B	1.7	14.10.2014	31.03.2015
1122	330,887	6,643,962	0.015 ± 0.001	Indoor (office)	B	1.7	14.10.2014	31.03.2015
1114	331,017	6,642,159	0.020 ± 0.001	Indoor (store)	MN	1.7	13.10.2014	31.03.2015
1105	332,008	6,641,917	0.0107 ± 0.0008	Outdoor (open shed)	MN	1.9	13.10.2014	31.03.2015
1118	331,955	6,641,485	0.0077 ± 0.0006	Outdoor (container)	MN	1.5	13.10.2014	31.03.2015
1112	331,955	6,641,485	0.105 ± 0.008	Indoor (office)	MN	1.9	13.10.2014	31.03.2015
1121	327,658	6,634,213	0.052 ± 0.004	Indoor (living room)	MS	1.7	13.10.2014	31.03.2015
1109	328,200	6,630,761	0.22 ± 0.02	Indoor (kitchen)	MS	1.6	13.10.2014	31.03.2015
1123	328,200	6,630,761	0.0087 ± 0.0006	Outdoor (open shed)	MS	1.9	13.10.2014	31.03.2015
1102	328,200	6,630,761	0.036 ± 0.001	Indoor (store)	MS	1.7	13.10.2014	31.03.2015

MN main north facies of the Piquiri Syenite Massif, *MS* main south facies of the Piquiri Syenite Massif, *B* border facies of the Piquiri Syenite Massif

[a]Height above ground floor

week; therefore, the relative exposure to Rn is decreased compared to other dwellings that are more frequently occupied. The office room identified by the detector 1112 is characterized by the constant use of air conditioner without a natural ventilation through windows. For other dwellings, no air conditioner was identified. In general, the living rooms for the studied dwellings were occupied mostly during afternoon and they were naturally ventilated by the opening of windows. However, this study did not include the winter season, where the ventilation conditions might be different. In sampling location of the detector 1109, placed in the kitchen, it was noticed that the rocks used as ornamental material are from the Piquiri syenitic massif.

The main north facies presents a mean outdoor and indoor Rn concentration of 0.009 kBq m^{-3} and 0.06 kBq m^{-3}, respectively, while the main south facies presents mean outdoor Rn concentration of 0.0087 kBq m^{-3} and indoor Rn concentration of 0.1 kBq m^{-3}, significantly higher than expected, taking into account that in the main south facies the predominant Rn isotope is ^{220}Rn, which cannot concentrate in the air without a high production rate. On the other hand, the mean outdoor and indoor Rn concentration in the border facies is 0.018 and 0.03 kBq m^{-3}. This facies has the lowest concentration of Rn in the soil (Romero-Mujalli and Roisenberg 2016), and the indoor measurements performed in this study suggest that this area represents lower risk to human health than compared to the main facies.

Results of the diffusion model

Figures 3, 4, and 5 are the simulations for border, main north and south facies, respectively. All figures show the Rn concentration at time 24 h of simulation; the deviation on Rn concentration due to random simulation is included.

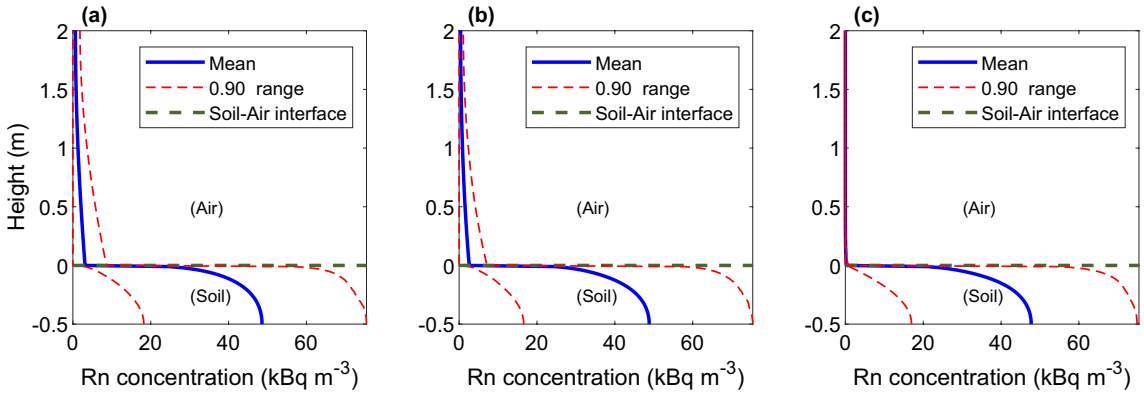

Fig. 3 Model results of the border facies (B) at time 24 h for 1000 random samples and three different simulation settings: (**a**) without ventilation rate, (**b**) ventilation rate (v) of 1×10^{-5} s^{-1}, and (**c**) simulation with ventilation rate (v) of 8×10^{-4} s^{-1}. Blue line stands for the average of 1000 samples, red lines represent the probability range of approximately 0.9 and green dash dot line represents the interface between soil and air

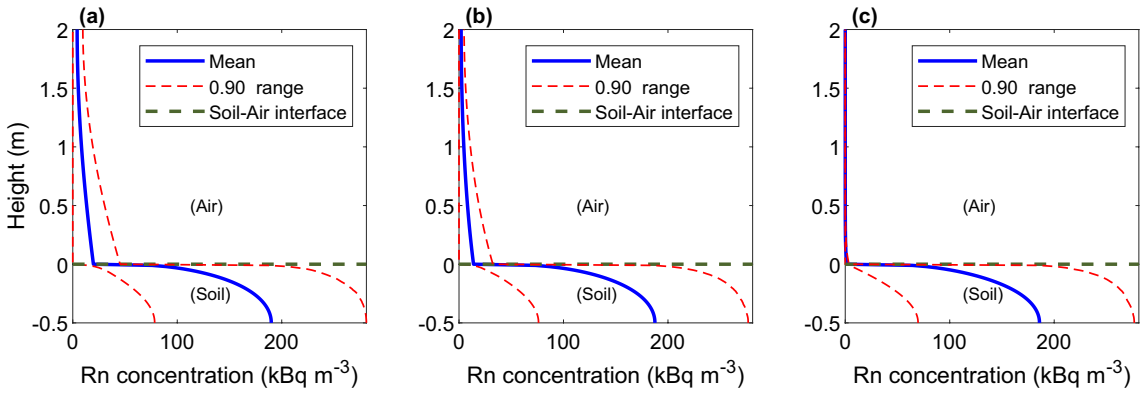

Fig. 4 Model results of the main north facies (MN) at time 24 h for 1000 random samples and three different simulation settings: (**a**) without ventilation rate, (**b**) ventilation rate (v) of 1×10^{-5} s^{-1}, and (**c**) simulation with ventilation rate (v) of 8×10^{-4} s^{-1}. Blue line stands for the average of 1000 samples, red lines represent the probability range of approximately 0.9 and green dash dot line represents the interface between soil and air

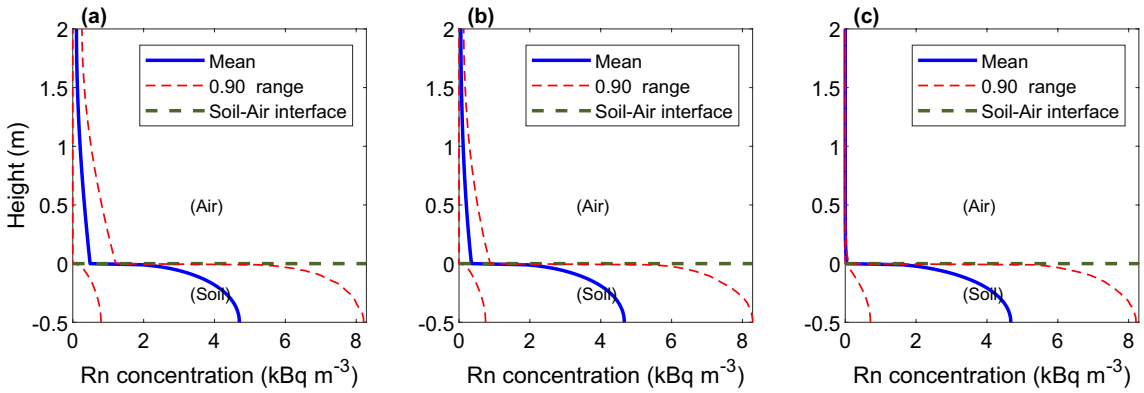

Fig. 5 Model results of the main south facies (MS) at time 24 h for 1000 random samples and three different simulation settings: (**a**) without ventilation rate, (**b**) ventilation rate (v) of 1×10^{-5} s^{-1}, and (**c**) simulation with ventilation rate (v) of 8×10^{-4} s^{-1}. Blue line stands for the average of 1000 samples, red lines represent the probability range of approximately 0.9 and green dash dot line represents the interface between soil and air

The different simulations conducted using the 1-D diffusion model described in Sect. 2.3 indicate that the time required to reach the reference air Rn concentration of 0.1 kBq m^{-3} depends, mainly, on the concentration of ^{222}Rn in the soil and the diffusion coefficient of the soil system, when no air exchange rate is considered. On the contrary, the simulations for ^{220}Rn indicates that this isotope does not accumulate in the air due to its fast decay kinetic. Moreover, the time required to reach a significant higher Rn concentration with respect to the reference value of 0.1 kBq m^{-3}, in a closed environment (without air exchange rate), is 10 ± 3 h, 7 ± 3 h and 16 ± 3 h for the border facies, main north facies and main south facies, respectively (Figs. 3a, 4a, 5a). In ill-ventilated environments, air exchange rate of 1×10^{-5} s^{-1}, the required time to arrive to the same reference value changes slightly to 10 ± 3 h, 8 ± 3 h and 18 ± 3 h for the border facies, main north facies and main south facies, respectively (Figs. 3b, 4b, 5b). Moreover, for high air exchange rate scenarios, air exchange rate of 8×10^{-4} s^{-1}, the Rn concentration in air decreases significantly, reaching a concentration comparable to the ones measured outdoor using the Rn detectors. Therefore, in all facies, the reference value of 0.1 kBq m^{-3} is not reached (Figs. 3c, 4c and 5c).

The significant larger time required to concentrate Rn in the air located in the main south facies (MS) is related, mainly, to the concentration of ^{222}Rn in the soil, because the soil diffusion coefficient estimated to this region is similar to the one in the MN. Furthermore, although randomly selected values, the higher soil moisture saturation in the border facies (B) with respect to the other syenitic facies leads to a lower soil diffusion coefficient, as represented by Eq. 5. Soil porosity might also display a strong control on diffusion coefficient. In this study, the same range of soil porosity was assumed for all syenitic facies.

Discussion

Outdoor radon concentrations in the study area present no risk to the health of the inhabitants compared to referenced levels. Indoor Rn concentrations, however, can be more than 10 times higher than the outdoor concentrations due to low ventilation and to Rn exhalation rate from ornamental material. The northern main facies of the syenitic massif presents the highest risk to human health compared to the other facies because of higher Rn concentrations in the soil. The high fracture densities observed in the field and in aerial photographs facilitate the transport of Rn from the soil to the atmosphere (Romero-Mujalli and Roisenberg 2016). This type of transport might be by advective fluids (Hoff 1997), facilitating the accumulation of Rn in ill-ventilated environments than the one that would have been calculated due to diffusive fluids. The results presented in this study support the application of modeling approaches to explore the potential indoor Rn concentration based on soil and dwelling characteristics, instead of the application of in situ indoor measurements that can be more expensive.

The significantly lower Rn concentrations in air with respect to the soil is the results of the difference on diffusion coefficient, which is given by the permeability and the water content in the soil, plus the removal of Rn in air due to the ventilation, parameters that strongly depend on weather conditions. Therefore, the Rn concentration in the air is transport controlled and the production and the destruction (the decay) of ^{222}Rn seem not to be the controlling factors as for the case of ^{220}Rn. The weather conditions did not vary

among sampling locations and no extreme event was record during the sampling campaign.

The main source of Rn into the buildings might be a combination of the transport from the soil and the exhalation of Rn from ornamental material. Specifically, indoor Rn concentrations increase by the use of ornamental rocks and the risk to human health will increase significantly in closed to ill-ventilated environments, as found in several studies (Chen et al. 2010; Moura et al. 2011; Amaral et al. 2015). The simulations conducted in this study demonstrate that the main mechanism to decreasing outdoor Rn concentration is the removal by wind ventilation, highlighting the importance of a well-ventilated environment for each day as a prevention technique.

The use of isolating materials at the bottom of the buildings can significantly reduce indoor Rn concentrations (Keller and Hoffmann 2000). For instance, one sample point (1118, Table 3), located inside a container in a mining area, presents low Rn concentration as compared to the indoor concentration in the office (1112, Table 3) with only few meters apart. In fact, this sample has the lowest air Rn concentration measured in this study. The low indoor Rn concentration in the container is mainly due to its composition, steel made, inhibiting the transport of Rn through its relative thin layer.

Despite that some studies have found that the less affluent homes present lower indoor Rn concentration than the more affluent ones in England (Kendall et al. 2016), in the study area, this case might not be applicable because most of the homes use the syenitic rocks as ornamental material. Moreover, in this region the use of air conditioner, which is common in the more affluent homes, can reduce indoor Rn concentrations (Lee and Yu 2000).

Indoor Rn concentrations can be potentially greater during winter due to ill-ventilated environments (Ramola et al. 1998; Kozak et al. 2011; Stojanovska et al. 2011). However, exhalation of Rn from the soil might be lower due to a lower soil temperature gradient (Dueñas et al. 1997). Another potential radiation sources with significant health risk are the ^{228}Ra and ^{226}Ra and ^{222}Rn concentration in groundwater (Schönhofer 1989; de Oliveira et al. 2001; Auvinen et al. 2002; Baykara and Dogru 2006). Natural waters of the Piquiri Syenite Massif, however not sampled in this study, are hypothesized to present relative high radioactive Ra and Rn concentrations. The Rn risk to human health, however not quantified in this study, should be determined by including the occupancy in dwellings and by measuring ventilation rate, which are key parameters in understanding the total exposure to Rn. Moreover, it is recommended that a survey of other radioactive species, e.g., radio (Ra), is conducted in the waters of the region.

The transport model developed in this study did not consider the advective transport due to ventilation, instead it considers a removal rate of Rn in air. The main limitation of the simulations conducted is that the random values taken for the soil moisture saturation and porosity carry a relatively high uncertainty in the result. Therefore, similar values were assumed for all syenitic facies, even though that the border facies (B) present a finer texture compared with the other facies. Moreover, although the relative air humidity in the soil is proportional to the soil moisture, its value cannot be converted directly. Furthermore, the boundary conditions between air and soil (Eq. 4) were estimated based on an explicit finite difference form.

Conclusions

The results obtained in this work show indoor Rn concentrations below the protective limit of 300 Bq m^{-3}, established by the International Atomic Energy Agency. Therefore, air radon in residences cannot be considered as a human health problem to the inhabitants of the area.

The diffusion model showed that there is a direct relationship between the ventilation condition of the room and the concentration of radon inside buildings, i.e., the indoor Rn concentrations can easily reach critical levels in confined or ill-ventilated environments. Moreover, the soil properties and soil moisture are, besides soil Rn concentration, important parameters controlling the transport and release of Rn to the atmosphere. The transport of radon from soil to dwellings depends on the composition and on defects in the structure of some materials (e.g., steel), as occurs in sample 1118, inhibiting the radon transport and accumulation.

Indoor Rn concentrations present a similar relationship with the syenitic facies as the one found for soils, with lower indoor Rn concentrations in dwellings located at the border facies, mainly due to differences in soil volumetric water content.

Acknowledgements The authors thank the Brazilian National Nuclear Energy Commission (CNEN) for the use of the equipment and the Rn detectors that supported this study. The authors thank the National Counsel Technological and Scientific Development (CNPq) for providing part of the funding necessary to develop this study.

Funding Open Access funding enabled and organized by Projekt DEAL.

Declarations

Conflict of interest The authors declare no competing interests.

References

Amaral P, Artur A, Bonotto D, Galembeck T (2015) Influence of dimension stones on the increase of radon gas levels indoors. KEM 634:548–558 (**Trans Tech Publ**)

Andersen CE (2001) Numerical modelling of radon-222 entry into houses: an outline of techniques and results. Sci Total Environ 272(1–3):33–42

Appleton J (2005) Radon in air and water essentials of medical geology: impacts of the natural environment on public health. In: Selinus O (ed) Elsevier. Amsterdam

Auvinen A, Kurttio P, Pekkanen J, Pukkala E, Ilus T, Salonen L (2002) Uranium and other natural radionuclides in drinking water and risk of leukemia: a case–cohort study in Finland. Cancer Causes Control 13(9):825–829

Baykara O, Dogru M (2006) Measurements of radon and uranium concentration in water and soil samples from East Anatolian Active Fault Systems (Turkey). Radiat Meas 41(3):362–367

Buffon SA (2002) Integração de dados geofísicos e geológicos na avaliação ambiental e epidemiológica de radiações naturais (radônio) no escudo Sul-Riograndense (RS-Brasil)

Casey JA, Ogburn EL, Rasmussen SG, Irving JK, Pollak J, Locke PA, Schwartz BS (2015) Predictors of indoor radon concentrations in Pennsylvania, 1989–2013. Environ Health Perspect 123(11):1130–1137

Castro MSMd, Vieira VA, Assunção RM (2004) Padrões espaço-temporais da mortalidade por câncer de pulmão no Sul do Brasil. Rev Bras Epidemiol 7:131–143

Chao CY, Tung TC, Burnett J (1997) Influence of ventilation on indoor radon level. Build Environ 32(6):527–534

Chen J, Rahman NM, Atiya IA (2010) Radon exhalation from building materials for decorative use. J Environ Radioact 101(4):317–322

de Oliveira J, Mazzilli BP, de Oliveira Sampa MH, Bambalas E (2001) Natural radionuclides in drinking water supplies of Sao Paulo State, Brazil and consequent population doses. J Environ Radioact 53(1):99–109

Dueñas C, Fernández M, Carretero J, Liger E, Pérez M (1997) Release of 222 Rn from some soils. Ann Geophys 15:124–133

Ferronsky V, Polyakov V (2012) Isotopes of the earth's hydrosphere. Springer Science & Business Media, Dordrecht

Fianco AC, Roisenberg A, Bonotto DM (2013) Radon emissions related to the granitic Precambrian shield in southern Brazil. Isot Environ Health Stud 49(1):122–131

Florică Ş, Burghele B-D, Bican-Brişan N, Begy R, Codrea V, Cucoş A, Catalina T, Dicu T, Dobrei G, Istrate A (2020) The path from geology to indoor radon. Environ Geochem Health 42(9):2655–2665

Haneberg WC, Wiggins A, Curl DC, Greb SF, Andrews WM Jr, Rademacher K, Rayens MK, Hahn EJ (2020) A geologically based indoor-radon potential map of Kentucky. GeoHealth. https://doi.org/10.1029/2020GH000263

Hartmann L, Chemale Jr F, Philipp R (2007) Evolução geotectônica do rio Grande do sul no pré-cambriano. Ianuzzi R. & Frantz JC.(Org.) 50: 97–123

Hoff A (1997) Radon transport in fractured soil. Laboratory experiments and modelling, Risoe National Lab

Instituto Nacional de Meteorologia (2020) INMET, Banco de Dados Meteorológicos Históricos Anuais. Disponível em: https://portal.inmet.gov.br/dadoshistoricos. Accessed on 25 Jan 2020

International Atomic Energy Agency (2014) Radiation protection and safety of radiation sources: international basic safety standards. International Atomic Energy Agency

Keller G, Hoffman B (2000) The radon diffusion length as a criterion for the radon tightness, IRPA10 conference proceedings, Hiroshima

Kendall GM, Miles JC, Rees D, Wakeford R, Bunch KJ, Vincent TJ, Little MP (2016) Variation with socioeconomic status of indoor radon levels in Great Britain: the less affluent have less radon. J Environ Radioact 164:84–90

Kozak K, Mazur J, Kozłowska B, Karpińska M, Przylibski T, Mamont-Cieśla K, Grządziel D, Stawarz O, Wysocka M, Dorda J (2011) Correction factors for determination of annual average radon concentration in dwellings of Poland resulting from seasonal variability of indoor radon. Appl Radiat Isot 69(10):1459–1465

Kukreja L, Bhawalkar D, Biswas S, Durgaprasad N, Kajarekar P, Vahia M, Yadav J, Basu C, Goswami J (1984) Cutting thin sheets of allyl diglycol carbonate (CR-39) with a CW CO2 laser: instrumentation and parametric investigation. Nucl Instrum Methods Phys Res 219(1):196–198

Lee TK, Yu K (2000) Effects of air conditioning, dehumidification and natural ventilation on indoor concentrations of 222Rn and 220Rn. J Environ Radioact 47(2):189–199

McGrath JA, Byrne MA (2020) An approach to predicting indoor radon concentration based on depressurisation measurements. Indoor Built Environ. https://doi.org/10.1177/1420326X20924747

Moura C, Artur A, Bonotto DM, Guedes S, Martinelli C (2011) Natural radioactivity and radon exhalation rate in Brazilian igneous rocks. Appl Radiat Isot 69(7):1094–1099

Nagda NL (1994) Radon: prevalence, measurements, health risks, and control. ASTM, West Conshohocken

Nardi L, Cid JP, Bitencourt M (2007) Minette mafic microgranular enclaves and their relationship to host syenites in systems formed at mantle pressures: major and trace element evidence from the Piquiri Syenite Massif, southernmost Brazil. Mineral Petrol 91(1–2):101–116

Nardi LV, Plá-Cid J, Bitencourt Md, Stabel LZ (2008) Geochemistry and petrogenesis of post-collisional ultrapotassic syenites and granites from southernmost Brazil: the Piquiri Syenite Massif. An Acad Bras Ciênc 80(2):353–371

Pereira J, Estrada J, Binns D, Urban M (1983) Técnica de Medida de Radônio no Ar Utilizando um Detector Plástico de Traços. IRD/CNEN. RJ

Philipp RP, Machado R, Nardi LVS, Lafon JM (2002) O magmatismo granítico Neoproterozóico do Batólito Pelotas no sul do Brasil: novos dados e revisão da geocronologia regional. Braz J Geol 32(2):277–290

Ramola R, Kandari M, Rawat R, Ramachandran T, Choubey V (1998) A study of seasonal variations of radon levels in different types of houses. J Environ Radioact 39(1):1–7

Rogers V, Nielson K (1991) Correlations for predicting air permeabilities and 222Rn diffusion coefficients of soils. Health Phys 61(2):225–230

Romero-Mujalli G, Roisenberg A (2016) Espectrometria de raios gama e emissão de radônio em solos da região do Maciço Sienítico Piquiri (Cachoeira do Sul e Encruzilhada do Sul, RS). Pesquisas Em Geociências 43(2):153–168

Santos CELd (2008) Determinação dos processos de enriquecimento e das concentrações de radônio em minas subterrâneas de fluorita e carvão do estado de Santa Catarina: critérios para avaliação dos riscos radiológicos

Schönhofer F (1989) Determination of radon-222 and radium-226 in mineral water and drinking water–a survey in Austria. Analyst 114(10):1345–1347

Sextro RG (1994) Radon and the natural environment. Radon: prevalence, measurement, health risks and control: 9–32

Silva AARd (2005) Radônio e filhos em residências da cidade de São Paulo, Universidade de São Paulo

Stojanovska Z, Januseski J, Bossew P, Zunic ZS, Tollefsen T, Ristova M (2011) Seasonal indoor radon concentration in FYR of Macedonia. Radiat Meas 46(6–7):602–610

Tunyagi A, Dicu T, Cucos A, Burghele B, Dobrei G, Lupulescu A, Moldovan M, Nită D, Papp B, Pap I (2020) An innovative system for monitoring radon and indoor air quality. Rom J Phys 65:803

USEPA (2016) A Citizen's Guide to Radon. U.S. Environmental Protection Agency (EPA). EPA402/K-12/002. Available: https://www.epa.gov/sites/production/files/2016-12/documents/2016_a_citizens_guide_to_radon.pdf. Accessed 27 Sept 2019

World Health Organization (2009) WHO handbook on indoor radon: a public health perspective. World Health Organization